



COLD BEAM INJECTION IN RELATIVISTIC EMEC WAVE FOR KAPPA DISTRIBUTION FUNCTION WITH AC FIELD FOR MAGNETO-PLASMA

R.S. Pandey¹, Rajbir Kaur^{1*}, K.M. Singh², B.N. Singh² and Vijay Prasad²

¹Department of Applied Physics, Amity Institute of Applied Sciences, Amity University, Noida Sector-125, India

rspandey@amity.edu

*Corresponding author: rkaur2@amity.edu

²Department of Physics, Veer Kunwar Singh University, Ara, Bihar, India

ABSTRACT

The effect of cold electron beam on electromagnetic electron cyclotron (EMEC) wave has been studied by using the unperturbed Lorentzian (Kappa) distribution in the magnetosphere for relativistic plasma. The dispersion relation is obtained by using the method of characteristic solutions and kinetic approach. An expression for the growth rate of a system has been calculated. It is inferred that in addition to the relativistic plasma obliquity and effect of cold electron beam modifies the growth rate and it also shifts the wave band significantly. The relativistic electrons by increasing the growth rate and widening the bandwidth may explain a wide frequency range of EMEC wave emissions in the magnetosphere.

Keywords:

Magnetosphere; Electron cyclotron waves; Kappa Distribution



Council for Innovative Research

Peer Review Research Publishing System

Journal: JOURNAL OF ADVANCES IN PHYSICS

Vol.7, No.1

www.cirjap.com , japeditor@gmail.com



INTRODUCTION

There is strong evidence that the high latitude ionosphere is an important source of magnetospheric ions, which is confirmed by the observations of the upward flowing accelerated ionospheric ions in the auroral zone. These upward flowing accelerated ionospheric ions can be characterized as either a beam like distribution of particles or conic like distribution depending upon their pitch angles.

In the last decade some authors have reported the presence of upward and downward flow of ions in the ionosphere [1-2]. Evidence for ion heating exists in the F-region where an intense super thermal ion beam was reported in confirmation with electrostatic ion-cyclotron wave observed near an auroral arc and was interpreted in terms of ion heating. Moreover different satellite observations have confirmed the presence of energetic (keV) up streaming ion beams and electrostatic waves in the magnetospheric plasma also. Penetration of ion beam in background plasma has been observed by various satellites and space probes. The ions accelerated towards the Earth's magnetotail far away from the Earth are reported to be of ionospheric origin.

Theoretical studies of whistler wave excitation have generally adopted anisotropic Maxwellian distributions to describe the resonant population. The dispersion relation can then be evaluated in terms of the plasma dispersion function [3]. However, in the natural space environment of planetary magnetospheres, astrophysical plasmas and the solar wind, plasmas are generally observed to possess a non-Maxwellian high energy tail component [4]. The origin of the high energy tail is not well understood, but once generated; the high energy tail persists in the collisionless magnetospheric environment. A useful distribution function to model such plasmas is the generalized Lorentzian (Kappa) distribution [5-6] explained by a spectral index κ and valid for $\kappa > 3/2$. The modified dispersion function (Kappa distribution) approaches the plasma dispersion function (Maxwellian) in the limit as $\kappa \rightarrow \infty$, although it can also be modeled by loss-cone distribution [7]. The modified dispersion function, Lorentzian (Kappa) distribution explains the wide spectrum range in comparison to bi-Maxwellian and loss-cone distribution functions. At the same time it is expected to be instrumental in studying micro instabilities in plasmas.

Kappa distribution has been used to analyze and interpret spacecraft data on the Earth's magnetospheric plasma sheet [4, 8], the solar wind [9], Jupiter [10] and Saturn [8]. In practice it is found that many space plasmas can be modeled more effectively by a superposition of Kappa distributions rather than by Maxwellians. In the context of both space and laboratory plasmas [11], it has been shown that the equilibrium state of the distribution function for a plasma immersed in superthermal radiation resembles a Lorentzian type distribution.

In the recent past whistler mode energetic electrons interaction assuming bi-Lorentzian (Kappa) particle distribution was studied by Thorne and Summers [12]. These authors derived the dispersion relation in the absence of AC electric field. These studies require the understanding of plasma properties subjected to fields of oscillating nature. In addition to injection of AC fields into space [13], electric field measurements at magnetospheric heights and in shock regions have given values of AC field along and perpendicular to Earth's magnetic field [14-15]. The behaviour of plasma in high frequency parallel and perpendicular AC fields have also been studied by a large number of investigators.

Motivated by these studies, in the present chapter, whistler mode instabilities have been analyzed for an anisotropic plasma having a generalized Lorentzian (Kappa) distribution function having spectral index κ , reducible to Maxwellian distribution in the limit $\kappa \rightarrow \infty$ in the presence of parallel AC electric field by method of characteristics solution. Using details of particle trajectories, dispersion relation and growth rate have been derived in analytical form and are evaluated for plasma parameters suited to the Earth's magnetosphere. Results have been discussed and compared with that obtained by earlier workers using Maxwellian distribution. It is observed that the Maxwellian and Kappa distributions differ substantially in the high energy tail, but the differences become less significant as κ increases.

MATHEMATICAL FORMULATION:

A spatially homogeneous anisotropic, collisionless plasma subjected to external magnetic field $\mathbf{B}_0 = B_0 \hat{e}_z$ and an electric field $\mathbf{E}_0 = E_0 \sin(\nu t) \hat{e}_x$ has been considered to get dispersion relation. In this case, linearized Vlasov-Maxwell equations, obtained after neglecting higher order terms and separating the equilibrium and non-equilibrium parts, following the technique of Pandey et al. [16], are given as below:

$$\mathbf{v} \cdot \left(\frac{\partial f_{s0}}{\partial \mathbf{r}} \right) + \frac{e_s}{m_s} \left[E_0 \sin(\nu t) + \left(\frac{\mathbf{v} \times \mathbf{B}_0}{c} \right) \right] \left(\frac{\partial f_{s0}}{\partial \mathbf{v}} \right) = 0 \quad (1)$$

$$\frac{\partial f_{s1}}{\partial t} + \mathbf{v} \cdot \left(\frac{\partial f_{s1}}{\partial \mathbf{r}} \right) + (F/m_s) \frac{\partial f_{s1}}{\partial \mathbf{v}} = \mathbf{S}(\mathbf{r}, \mathbf{v}, t) \quad (2)$$

Where force is given as $F = m \frac{dv}{dt}$



$$\mathbf{F} = e_s \left[E_0 \sin(\nu t) + \left(\frac{\mathbf{v} \times \mathbf{B}_0}{c} \right) \right] \tag{3}$$

The particle trajectories are obtained by solving equation of motion defined in equation (3) and $S(r, \nu, t)$ is defined as:

$$S(\mathbf{r}, \mathbf{v}, t) = -(e/m_s) \left[E_1 + \left(\frac{\mathbf{v} \times \mathbf{B}_1}{c} \right) \right] \left(\frac{\partial f_{s0}}{\partial \mathbf{v}} \right) \tag{4}$$

where s denotes species and E_1 , B_1 and f_{s1} are perturbed quantities and are assumed to have harmonic dependence in E_1 , B_1 and $f_{s1} = \exp i(\mathbf{k} \cdot \mathbf{r} - \omega t)$. The method of characteristic solution is used to determine the perturbed distribution function, f_{s1} , which is obtained from Eq. (2) by

$$f_{s1}(\mathbf{r}, \mathbf{v}, t) = \int_0^\infty s \{ \mathbf{r}_0(\mathbf{r}, \mathbf{v}, t'), \mathbf{v}_0(\mathbf{r}, \mathbf{v}, t'), t - t' \} dt' \tag{5}$$

The phase space coordinate system has been transformed from $(\mathbf{r}, \mathbf{v}, t)$ to $(\mathbf{r}_0, \mathbf{v}_0, t - t')$. The particle trajectories which are obtained by solving eq. (3) for the given external field and wave propagation, $\mathbf{k} = [k_\perp \hat{e}_x, 0, k_\parallel \hat{e}_z]$ are:

$$\begin{aligned} X_0 &= X + \left(\frac{P_\perp \sin \theta}{\omega_{cs} m_s} \right) - \left[P_\perp \sin \left\{ \theta + \left(\frac{\omega_{cs} t}{\gamma} \right) \right\} \right] + \left[\frac{\Gamma_{xs} \sin \nu t}{\gamma \left\{ \left(\frac{\omega_{cs}}{\gamma} \right)^2 - \nu^2 \right\}} \right] - \left[\frac{\nu \Gamma_{xs} \sin \left(\frac{\omega_{cs} t}{\gamma} \right)}{\omega_{cs} \left\{ \left(\frac{\omega_{cs}}{\gamma} \right)^2 - \nu^2 \right\}} \right] \\ Y_0 &= Y - \left(\frac{P_\perp \cos \theta}{\omega_{cs} m_s} \right) + \left[P_\perp \cos \left\{ \theta + \left(\frac{\omega_{cs} t}{\gamma} \right) \right\} \right] + \left(\frac{\Gamma_{xs}}{\nu \omega_{cs}} \right) - \frac{\left\{ 1 + \nu^2 \beta^2 \cos \left(\frac{\omega_{cs} t}{\gamma} \right) - \omega_{cs}^2 \cos \nu t \right\}}{\gamma^2 \left\{ \left(\frac{\omega_{cs}}{\gamma} \right)^2 - \nu^2 \right\}} \\ Z_0 &= Z - \frac{P_z}{\lambda m_s} \end{aligned} \tag{6}$$

and the velocities are

$$\begin{aligned} v_{x0} &= P_\perp \cos \left\{ \theta + \left(\frac{\omega_{cs} t}{\gamma} \right) \right\} + \left[\frac{\nu \Gamma_{xs}}{\gamma \left\{ \left(\frac{\omega_{cs}}{\gamma} \right)^2 - \nu^2 \right\}} \right] \left\{ \cos \nu t - \cos \left(\frac{\omega_{cs} t}{\gamma} \right) \right\} \\ v_{y0} &= P_\perp \sin \left\{ \theta + \left(\frac{\omega_{cs} t}{\gamma} \right) \right\} + \left[\frac{\Gamma_x}{\gamma \left\{ \left(\frac{\omega_{cs}}{\gamma} \right)^2 - \nu^2 \right\}} \right] \left\{ \left(\frac{\omega_{cs}}{\gamma} \right) \sin \nu t - \nu \sin \left(\frac{\omega_{cs} t}{\gamma} \right) \right\} \end{aligned} \tag{7}$$

$$v_{z0} = \frac{P_z}{\gamma m_s}, \quad v_x = \frac{P_\perp \cos \theta}{\gamma m_s}, \quad v_y = \frac{P_\perp \sin \theta}{\gamma m_s}, \quad v_z = \frac{P_z}{\gamma m_s}$$



$$m_s = \frac{m_{0s}}{\gamma}, \quad \omega_{cs} = \frac{e_s B_0}{m_s}, \quad \gamma = \sqrt{1 - \frac{v^2}{c^2}}, \quad \Gamma_{xs} = \frac{e_s E_0}{m_s}$$

P_{\perp} and P_z denote momenta perpendicular and parallel to the magnetic field. Using equations (5), (6) and the Bessel identity and performing the time integration, following the technique and method of Pandey and Kaur [17], the perturbed distribution function is found after some lengthy algebraic simplifications as :

$$f_{s1} = - \left(\frac{ie_s}{m_s \gamma \omega} \right) \sum J_s(\lambda_3) \exp(i(m-n)\theta) \left[\frac{J_m J_n J_p U^* E_{1x} - i J_m V^* E_{1y} + J_m J_n J_p W^*}{\omega - \left(\frac{k_{\parallel} P_z}{\gamma m_s} + p v - \frac{(n+g)\omega_{cs}}{\gamma} \right)} \right]$$

Due to the phase factor the solution is possible when $m = n$. Here

$$U^* = \left(\frac{c_{\perp} P_{\perp} n}{\gamma \lambda_1 m_s} \right) - \left(\frac{m v c_{\perp} D}{\lambda_1} \right) + \left(\frac{p v c_{\parallel} D}{\lambda_2} \right), \quad V^* = \left(\frac{c_{\perp} P_{\perp} J_n J_p}{\gamma m_s} \right) + c_{\parallel} D J_p J_n \omega_{cs}$$

$$W^* = \left(\frac{n \omega_{cs} F m_s}{k_{\perp} P_{\perp}} \right) + \left(\gamma m_s P_{\perp} \omega \frac{\partial f_0}{\partial P_z} \right) + G \left\{ \left(\frac{p}{\lambda_2} \right) - \left(\frac{n}{\lambda_1} \right) \right\}$$

$$C_1 = \left\{ \frac{(\gamma m_s)}{P_{\perp}} \right\} \left(\frac{\partial f_0}{\partial P_{\perp}} \right) \left(\omega - \frac{k_{\parallel} p_z}{\gamma m_s} \right) + k_{\parallel} \gamma m_s \left(\frac{\partial f_0}{\partial P_{\perp}} \right)$$

(8)

$$D = \frac{\Gamma_{xs}}{\gamma \left\{ \left(\frac{\omega_{cs}}{\gamma} \right)^2 - v^2 \right\}}, \quad F = \frac{H k_{\perp} P_{\perp}}{\gamma m_s}, \quad H = \left\{ \frac{(\gamma m_s)^2}{P_{\perp}} \right\} \left(\frac{\partial f_0}{\partial P_{\perp}} \right) \left(\frac{P_z}{\gamma m_s} \right) + \gamma m_s \left(\frac{\partial f_0}{\partial P_z} \right)$$

$$G = \frac{H k_{\perp} v \Gamma_{xs}}{\gamma \left\{ \left(\frac{\omega_{cs}}{\gamma} \right)^2 - v^2 \right\}}, \quad J_n(\lambda_1) = \frac{dJ_n(\lambda_1)}{d\lambda_1}, \quad J_p(\lambda_2) = \frac{dJ_p(\lambda_2)}{d\lambda_2} \text{ and the Bessel function arguments are defined as}$$

$$\lambda_1 = \frac{k_{\perp} P_{\perp}}{\omega_{cs} m_s}, \quad \lambda_3 = \frac{k_{\perp} v \Gamma_{xs}}{\gamma \left\{ \left(\frac{\omega_{cs}}{\gamma} \right)^2 - v^2 \right\}}, \quad \lambda_2 = \frac{k_{\perp} \Gamma_{xs}}{\gamma \left\{ \left(\frac{\omega_{cs}}{\gamma} \right)^2 - v^2 \right\}}$$

The conductivity tensor is written as $\|\sigma\| = \frac{-i \sum (e_s^2 / m_s \lambda)^2 \omega \int d^3 P J_g(\lambda_3) \|s\|}{\left[\omega - \left(\frac{k_{\parallel} P_z}{\gamma m_s} \right) - \left(\frac{(n+g)\omega_{cs}}{\gamma} \right) + p v \right]}$ (9)

$$\text{Where } \|S\| = \begin{vmatrix} P_{\perp} J_n^2 J_p \left(\frac{n}{\lambda_1} \right) U^* & i P_{\perp} J_n V^* & P_{\perp} J_n^2 J_p \left(\frac{n}{\lambda_1} \right) W^* \\ i P_{\perp} J_n' J_n J_p \left(\frac{n}{\lambda_1} \right) U^* & P_{\perp} J_n' V^* & i P_{\perp} J_n' J_n J_p \left(\frac{n}{\lambda_1} \right) W^* \\ P_z J_n^2 J_p \left(\frac{n}{\lambda_1} \right) U^* & i P_z J_n V^* & P_z J_n^2 J_p \left(\frac{n}{\lambda_1} \right) W^* \end{vmatrix}$$

(10)



By using these in the Maxwell's equations we get the dielectric tensor,

$$\epsilon_{ij} = 1 + \sum \left\{ \frac{4\pi e_s^2}{(\gamma m_s)^2 \omega} \right\} \int \frac{d^3 P J g(\lambda_3) \| S \|}{\left(\omega - \frac{k_{\parallel} P_z}{\gamma m_s} \right) - \left\{ \frac{(n+g)\omega_{cs}}{\gamma} \right\} + p v} \quad (11)$$

For parallel propagating whistler mode instability, the general dispersion relation reduces to

$$\epsilon_{11} \pm \epsilon_{12} = N^2, \quad N^2 = \frac{k^2 c^2}{\omega^2} \quad (12)$$

The dispersion relation for relativistic case with perpendicular AC electric field for $g=0, p=1, n=1$ is written as:

$$\frac{k^2 c^2}{\omega^2} = 1 + \frac{4\pi e_s^2}{(\gamma m_s)^2 \omega^2} \int \frac{d^3 P}{\gamma} \left[\frac{P_{\perp}}{2} - \frac{v \Gamma_{xs} m_s}{2 \left(\frac{\omega_{cs}^2}{\gamma^2} - v^2 \right)} \right] \left[\left(\gamma \omega - \frac{k_{\parallel} P_{\parallel}}{m_s} \right)^2 \frac{\partial f_0}{\partial P_{\perp}} + \frac{P_{\perp} k_{\parallel}}{m_s} \frac{\partial f_0}{\partial P_{\parallel}} \right] \frac{1}{\gamma \omega - \frac{k_{\parallel} P_{\parallel}}{m_s} - \omega_{cs} + \gamma v} \quad (13)$$

The unperturbed Lorentzian-Kappa distribution function is:

$$f_0 = \frac{n_0}{\pi^{3/2} P_{0\perp}^2 P_{0\parallel} k^{3/2}} \frac{\Gamma(k+1)}{\Gamma(k+1/2)} \left[1 + \frac{P_{\parallel}^2}{k P_{0\parallel}^2} + \frac{P_{\perp}^2}{k P_{0\perp}^2} \right]^{-(k+1)} \quad (14)$$

And associated parallel and perpendicular effective thermal speeds are

$$P_{0\parallel} = \left[\frac{2k-3}{k} \right]^{1/2} \left(\frac{T_{\parallel s}}{m_s} \right)^{1/2}, \quad P_{0\perp} = \left[\frac{2k-3}{k} \right]^{1/2} \left(\frac{T_{\perp s}}{m_s} \right)^{1/2}$$

Applying the approximation in electron-cyclotron range of frequencies. In this case, ion temperature are assumed $T_{is} = T_{i\parallel} = T_i$ and assumed to be magnetized with $|\omega_r + i\gamma| \ll \omega_{cs}$ while electrons are assumed to have $T_{\perp e} > T_{\parallel e}$ and $|k_{\parallel} \alpha_{\parallel}| \ll |\omega_r \pm \omega_{cs} + i\gamma|$ for background plasma. Therefore Equation (13) becomes the following, as a sum of background and injected cold beam plasma:

$$D(k, \omega_r + i\gamma) = 1 - \frac{k^2 c^2}{\omega_r + i\gamma} + \sum \frac{J_p(\lambda_2) J_q(\lambda_3)}{\alpha_{\perp s}^2} \left[\left\{ \frac{\omega_i^2}{\omega_{ce}^2} - \frac{\omega_{pi}^2}{(\omega_r + i\gamma) \pm \omega_{ce}} \right\} \left\{ X_i \frac{\omega_{pi}^2}{(\omega_r + i\gamma)} \right\} \frac{\omega_r + i\gamma}{k_{\parallel} \theta_{\parallel e}} \left(\frac{k-1}{k} \right)^{1/2} \right] \times \left[\left(\frac{k-1}{k-3/2} \right) Z_{k-1} \left(\left(\frac{k-1}{k} \right)^{1/2} \xi_e \right) A_T \left\{ 1 + \xi_e \left(\left(\frac{k-1}{k} \right)^{1/2} \left(\frac{k-1}{k-3/2} \right) Z_{k-1}^* \left(\frac{k-1}{k} \right)^{1/2} \xi_e \right) \right\} \right] - \frac{\omega}{\omega \pm \omega_c} \frac{\omega_{pc}^2}{\omega_{pw}^2} \quad (20)$$

Where $X_{li} = \theta_{li}^2 - \frac{v \Gamma_{xi}}{\omega_{ci}^2 - v^2} \frac{\theta_{li}}{2} \sqrt{\pi}$

$$X_{le} = \theta_{le}^2 - \frac{v \Gamma_{xe}}{\omega_{ce}^2 - v^2} \frac{\theta_{le}}{2} \sqrt{\pi}$$

$$A_T = \frac{\theta_{\perp e}^2}{\theta_{\parallel e}^2} - 1$$

$Z(\xi) =$ Plasma Dispersion Function



here the function $Z_{\kappa-1}^*$ occurring in Eq. (21) is the modified plasma dispersion function defined by Summers and Thorne [8].

$$Z_{\kappa}^*(\xi) = \frac{1}{\sqrt{\pi}} \frac{\Gamma(\kappa-1)}{\kappa^{3/2} \Gamma(\kappa-1/2)} \int_{-\infty}^{\infty} \frac{ds}{(s-\xi)(1+s^2/\kappa)} \kappa+1 \quad \dots(18)$$

$\text{Im}(\xi) > 0$ The power series $Z_{\kappa}^*(\xi)$ is given by

$$Z_{\kappa}^*(\xi) = \frac{i\kappa! \kappa^{(\kappa-1/2)} \sqrt{\pi}}{\Gamma(\kappa-1/2) \xi^{2(\kappa+1)}} \left(1 - \frac{\kappa(\kappa+1)}{\xi^2} + \dots \right) - \left(\frac{2\kappa-1}{2\kappa} \right) \frac{1}{\xi} \left[1 + \left(\frac{\kappa}{2\kappa-1} \right) \frac{1}{\xi^2} + \dots \right]$$

For $(\xi) \longrightarrow \infty$... (19)

Applying condition $\frac{k^2 c^2}{\omega^2} \gg 1 + \frac{\omega_{pi}^2}{\omega_{ci}^2}$ with $p=1, n=1$ and $q=0$ we can get the growth rate and real frequency

using $K_3 = 1 - \gamma X_3 + \gamma X_4, K_4 = \frac{\gamma X_3}{1 - \gamma X_3 + \gamma X_4},$

$$\tilde{k} = \frac{k_{||} \alpha_{||}}{\omega_{cs}}, \quad \beta = \frac{K_B T_{||} \mu_o n_o}{B_o^2}, \quad \Gamma_{xs} = \frac{e E_o}{m_s}, \quad X_4 = \frac{-\gamma v}{\omega_{ce}}, \quad \delta = 1 + \frac{n_c}{n_w} (1 + \gamma X_4)$$

When EMEC waves propagate parallel to magnetic field direction, the expression of growth rate and real frequency becomes:

$$\frac{\gamma}{\omega_{ce}} = \frac{\frac{\sqrt{\pi}}{\gamma \tilde{k}} \left(\frac{(k-1)! k^{k-1/2}}{(k-3/2)!} \right) (A_T - K_4) K_3^3 \left\{ - \left(\frac{k^3}{\tilde{k}} \right) \right\}^{-2k}}{1 + \gamma X_4 + \frac{k}{k-3/2} \left[\frac{(1 + \gamma X_4) \tilde{k}^2}{2 K_3^2} + \frac{\tilde{k}^2}{K_3} (A_T - K_4) \right] - \frac{X_{1e}}{X_{1i}} K_3^2 + \frac{(\delta-1) K_3^2}{(1-X_3)^2 (1 + \gamma X_4)}} \quad (21)$$

$$X_3 = \frac{\omega_r}{\omega_{ce}} = \frac{\tilde{k}^2}{\gamma \delta \beta} \left[\frac{X_{1e} (1 + \gamma X_4)}{X_{1e} - X_{1i} (1 + \gamma X_4)} + \frac{A_T \beta X_{1e}}{2(1 + \gamma X_4) (X_{1e} - X_{1i} (1 + \gamma X_4))} \right] \quad (22)$$

DISCUSSION:

Plasma Parameters:

To study the variation of dimensionless growth rate of electromagnetic electron-cyclotron waves consisting of kappa distribution function, following plasma parameters have been considered $B_0 = 1 \times 10^{-7} T, E_o = 4 \text{ mV/m}, k_B T_{||i} = 100 \text{ eV}, k_B T_{||e} = 5 \text{ KeV}, T_{\perp}/T_{||} = 1.25, 1.5, 1.75, \nu = 2 \text{ KHz}, 3 \text{ KHz}, 4 \text{ KHz}, \gamma = 0.5, 0.6, 0.7$ and $n_c/n_w = 10, 15, 20, 30$. According to this choice of plasma parameters, the discussion of the results is given as.

Results:

Figure 1 shows the variation of growth rate and real frequency with respect to \tilde{k} for various values of temperature anisotropy A_T of background plasma and other fixed parameters as listed in figure caption. Since $A_T = [(T_{\perp}/T_{||}) - 1]$, A_T becomes 0.25, 0.50 and 0.75. For $T_{\perp}/T_{||} = 1.25, 1.5$ and 1.75 , the growth rate is 0.00389, 0.0053 and 0.0062 respectively. The maxima changes from $\tilde{k} = 0.22$ to $\tilde{k} = 0.23$ and $\tilde{k} = 0.23$. As the value of A_T increases, growth rate increases. In this graph the growth rate increases with increase of temperature anisotropy and maxima is shifted significantly towards the higher k values. It is clear from the figure that the temperature anisotropy is the main source of energy to drive the

excitation of the wave. The real frequency increases with increasing value of \tilde{k} . This satisfied the condition of electromagnetic waves. In **figure2** variation of dimensionless growth rate and real frequency with respect to \tilde{k} for various values of AC frequencies is shown with other fixed parameters as mentioned in figure caption. The growth rate is 0.00516, 0.00630 and 0.00812 for $\nu = 2$ KHz, 3 KHz and 4 KHz at $\tilde{k} = 0.24$, $\tilde{k} = 0.23$ and $\tilde{k} = 0.22$ respectively. It is seen that growth rate increases with increase in AC frequency but maxima shifts to lower value of wave number. The real frequency increases with increasing value of \tilde{k} . This satisfied the condition of electromagnetic waves. **Figure 3** shows the variation of growth rate and real frequency with \tilde{k} for various values of ratio of number density of cold electrons to hot electrons. The number density of hot background plasma is assumed variable as $5 \times 10^6 \text{m}^{-3}$, $2.5 \times 10^6 \text{m}^{-3}$ and $1.6 \times 10^6 \text{m}^{-3}$, thus giving n_c/n_w as 10, 20 and 30 (approximately). The growth rate is 0.0051 for $n_c/n_w = 10$ at $\tilde{k} = 0.24$, the growth rate is 0.0058 when $n_c/n_w = 20$ at $\tilde{k} = 0.28$ and growth rate is $\gamma/\omega_c = 0.0067$ for $n_c/n_w = 30$ at $\tilde{k} = 0.33$. This shows that as the number density of hot electrons decreases, that is, as the ratio of n_c/n_w increases from 10 to 30, growth rate increases. The increase in bandwidth and significant shift in \tilde{k} values also seen in graph from 0.24 to 0.33 for kappa distribution index $\kappa = 2$. The real frequency increases with increasing value of \tilde{k} . This satisfied the condition of electromagnetic waves. Results can be compared with Pandey et al. [18] Lorentzian/Kappa plasma series expansion brings change in thermal velocity (perpendicular), affecting terms of temperature anisotropy. Temperature anisotropy being the primary source of instability gets further modified by Kappa distribution function, giving rise to further increase in growth rate. The theory of kappa distribution also explains that suprathermal electron in Kappa distribution modifies the intensity and Doppler frequency of electron plasma. The inclusion of temperature anisotropy in Lorentzian (Kappa) plasma can explain the observed higher frequencies spectrum of whistler waves [17, 19]. **Figure 4** shows the variation of growth rate and real frequency with respect to \tilde{k} for various values of relativistic factor of background plasma and other fixed parameters as listed in figure caption. In this graph the growth rate increases with increase of relativistic factor and maxima is fixed for \tilde{k} values. It is clear from the figure that the relativistic factor is the source of energy to drive the excitation of the wave. The real frequency increases with increasing value of \tilde{k} . This satisfied the condition of electromagnetic waves.

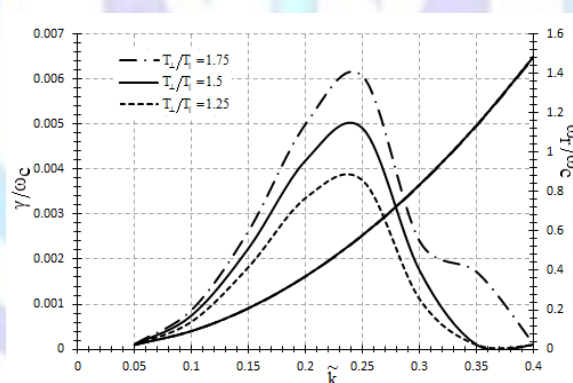


Fig 1. Variation of Growth Rate and Real Frequency with respect to \tilde{k} for various values T_{\perp}/T_{\parallel} at $n_o=4 \times 10^4 \text{m}^{-3}$, $\gamma = 0.5$, $\nu = 2 \text{Hz}$ and other fixed plasma parameters.

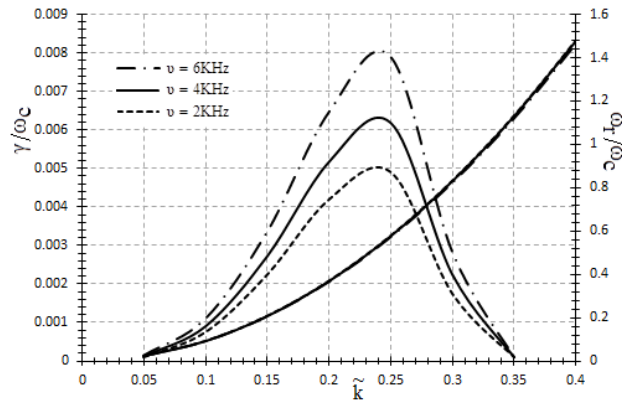


Fig 2. Variation of Growth Rate and Real Frequency with respect to \tilde{k} for various values of AC frequency ν , at $T_{\perp}/T_{\parallel} = 1.25$, $\gamma = 0.5$, $n_o = 4 \times 10^4 \text{m}^{-3}$ and other fixed plasma parameters.

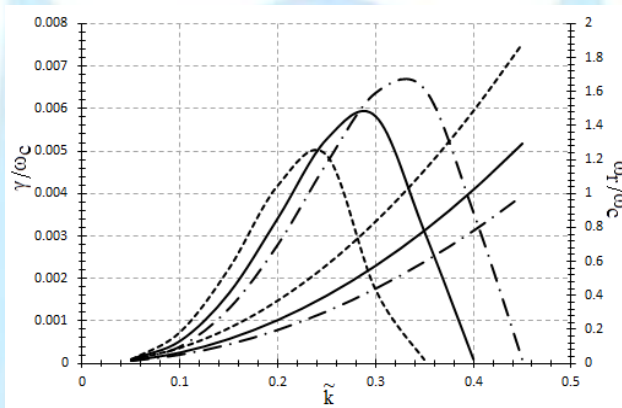


Fig.3. Variation of Growth Rate and Real Frequency with respect to \tilde{k} for various values of n_o/n_w at $T_{\perp}/T_{\parallel} = 1.25$, $\gamma = 0.5$, $n_o = 4 \times 10^4 \text{m}^{-3}$ and other fixed plasma parameters.

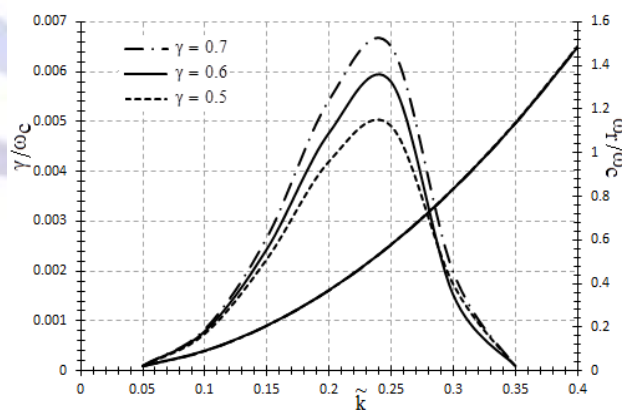


Fig 4. Variation of Growth Rate and Real Frequency with respect to \tilde{k} for various values of γ at $n_o/n_w = 10$, $T_{\perp}/T_{\parallel} = 1.25$, $n_o = 4 \times 10^4 \text{m}^{-3}$ and other fixed plasma parameters.



REFERENCES

- [1] Keating, J.G., Mulligan, F.J., Doyle, D.B., Winser, K.J. and Lockwood, M., 1990, Planet Space Sci. 38,1187
- [2] Yeh, H.C. and Foster, J.E., 1990, J. Geophys. Res, 95, 7881
- [3] Fried, B. D. and Conte, S. D., 1961, Academic San Diego, Calif. (USA)
- [4] Williams D. J., Mitchell, D. G. & Criston, S. P., 1988, J. Geophys. Res. Lett. 15, 303.
- [5] Christon, S. P., Mitchell, D. G., Williams, D. J., Frank, L.A., Huang, C. Y. & Eastman, T. E., 1988, J. Geophys. Res. 93, 2568.
- [6] Christon, S.P., Williams, D. J. & Mitchell, D. G, 1991, J. Geophys. Res. 96,1.
- [7] Thorne, R.M. and Summers D., 1992, Geophys. Res. Lett., 19, 417.
- [8] Summers, D. & Thorne, R.M., 1991, Phys. Fluids 3, 1835
- [9] Gosling, J. T., Asbridge, J.R., Bame, S. J., Feldman, W. C., Zwickl, R.D., Paschman, G., Sokopke, N., & Hynds, R. J., 1981, J. Geophys. Res. 86, 547.
- [10] Lyons, L. T. & Thorne, R. M., 1972, J. Geophys. Res. 77, 5608.
- [11] Hasegawa, A., Mima, K., & Doung-Van. M., 1985, Phys. Rev. Lett., 54, 2608.
- [12] Thorne, R. M., and Horne R. B., 1996, J. Geophys. Res., 101, 4917.
- [13] Inan U.S., Bell, T.F., Carpender ,D.L. and Anderson ,R.R., 1977, J. Geophys. Res., 82, 1177
- [14] Misra, K.D. and Haile, T., 1993, J. Geophys Res., 98, 9297
- [15] Misra K.D. and Pandey, R.S., 1995, J. Geophys Res., 100, 19405
- [16] Pandey R.S. and Misra K.D., 2002, Earth Planets Space, 54, 159
- [17] Pandey R.S. and Rajbir Kaur, 2012, Progress in Electromagnetics Research B 45, 337.
- [18] Pandey, R.P., Karim S.M., Singh K.M., and Pandey R.S., 2002, Earth Moon and Planets, Vol. 91, 195
- [19] Pandey R. S., Pandey R. P., Karim, S.M., Srivasta A.K. and Hariom, 2008, Progress in Electromagnetics Research M, 1, 207